

associated with ferricyanide sites.

The absorbance spectrum of the partially oxidized film (0.755 V) is intermediate between those of the fully oxidized and reduced film, except for an increase in the near-infrared portion of the spectrum (at wavelengths greater than 900 nm). The absorption increase in this region is reproducible, but its origin is uncertain. Since the voltammetric data suggest that two oxidation processes occur in VHCF, this absorption band may arise from VHCF that has undergone only the first oxidation step. The lack of an isosbestic point in Figure 6 is consistent with the presence of at

least two oxidation processes for VHCF.

Acknowledgment. We are grateful to Michael Balogh and Audrey Dow for ICP measurements and XPS data collection, respectively. We also thank G. A. Nazri for helpful discussions and the Watkins-Johnson Co. (Scotts Valley, CA) for their donation of FTO-coated glass substrates.

Registry No. VHCF, 89184-12-3; TO, 18282-10-5; F₂, 7782-41-4; Pt, 7440-06-4; Na₃VO₄, 13721-39-6; K₃Fe(CN)₆, 13746-66-2; K₂SO₄, 7778-80-5; H₂SO₄, 7664-93-9.

Contribution from the Department of Chemistry,
North Dakota State University, Fargo, North Dakota 58105

Relationship of the Ruby Spectrum to the Geometry of the Chromium(III) Environment

Kyu-Wang Lee and Patrick E. Hoggard*

Received July 12, 1988

The electronic spectrum of ruby has been fit by using the angular overlap model (AOM) to express the total ligand field potential at the Cr³⁺ site from the nearest 813 oxide ions and 542 aluminum ions. The optimized AOM parameter values were $e_{\sigma O} = 8867 \text{ cm}^{-1}$ and $e_{\pi O} = 853 \text{ cm}^{-1}$ for the oxide ions nearest to the chromium and $e_{\sigma Al} = -9275 \text{ cm}^{-1}$ for the nearest Al³⁺, with $e_{\pi Al}$ fixed at zero. The oxide ion AOM parameters were constrained to decline with the distance from Cr³⁺ as R^{-3} , while $e_{\sigma Al}$ was reduced as R^{-3} . The relatively small value of $e_{\pi O}$ results from a distribution of the oxide ion electron donor properties among a distorted tetrahedron of aluminum ions.

Introduction

The electronic structure of ruby (Cr³⁺ doped in α -alumina) is of both historical and practical interest, and a considerable effort has been invested in the measurement of the transition energies to the d-d excited states and in the use of ligand field theory to calculate these transition energies, beginning with the pioneering work of Sugano et al.¹⁻³ on the effects of a trigonally distorted crystal field. The electronic spectrum of ruby is more completely and more accurately known than that of any other Cr(III) system,⁴⁻¹³ with the exception of the free ion, and thus constitutes a particularly important challenge to ligand field theory.

All previous treatments have been based on the actual C_{3v} or approximate C_{3h} symmetry of the Cr³⁺ ion site, and the one-electron ligand field potential matrix has been developed from a generalized trigonal potential, which may be expressed as the sum of an octahedral potential and additional terms allowed in the trigonal symmetry.^{14,15} The ligand potential matrix, $\langle d_i | V | d_j \rangle$, has a minimum of four unrelated nonzero elements, which may be expressed by using C₃ (O_h) labels for the d orbitals as $\langle e(t_2) | V | e(t_2) \rangle$, $\langle e(e) | V | e(e) \rangle$, $\langle e(t_2) | V | e(e) \rangle$, and $\langle a_1(t_2) | V | a_1(t_2) \rangle$. Since only energy differences are observed, one of these is arbitrary, and the trigonal field can be evaluated with three parameters. Generally these are chosen as an octahedral parameter Δ , equal to the energy difference between $e(e_g)$ and the center

of gravity of the t_{2g} orbitals, and two trigonal perturbation terms, one representing the (diagonal) splitting within the t_{2g} orbitals, and the other, sometimes neglected,¹ the off-diagonal element $\langle e(t_2) | V | e(e) \rangle$.

In their attempt to model the ruby spectrum, Sugano and Peter started with nine parameters: the three ligand field parameters, two spherical interelectronic repulsion parameters (the Racah parameters B and C), two spin-orbit coupling parameters (one between t_{2g} orbitals and one between a t_{2g} and an e_g orbital), and two orbital reduction parameters, defined like the spin-orbit coupling parameters.³ This set of parameters was effectively reduced by two by the assumption that the pairs of trigonal field, spin-orbit coupling, and orbital reduction parameters stand in the same relationship. It was further reduced to a total of six adjustable parameters by fixing the value of C at 4B. The secular determinants were derived only from the t_{2g} and t_{2g}²e_g configurations, and no optimization procedure was used to find the global minimum. The orbital reduction factors k and k' were used in the magnetic field dependent portion of the Hamiltonian.¹⁶ Normally these parameters would affect only the g values determined from Zeeman splittings, but by being subjected to a relationship with the spin-orbit coupling and trigonal field parameters, the value of k also affected the zero-field transition energies. The calculations were applied only to states from the t_{2g}³ configuration, including the zero-field splitting (ZFS) of the ⁴A_{2g} ground state, and their results are shown in Table I.

Macfarlane in 1963 improved on this calculation by including all configurations in setting up the secular determinant.¹⁷ Although final energy eigenvalues were determined by diagonalizing the matrices within each C_{3v}* double-group representation, parameter refinement had to be carried out by means of perturbation expressions. The six-parameter set used by Macfarlane consisted of the three ligand field parameters, the Racah parameters B and C, and a single spherical spin-orbit coupling parameter. The results, shown in Table I, reproduce the sharp-line splittings rather well, although the term energies themselves are not nearly as well fit.

- (1) Sugano, S.; Tanabe, Y. *J. Phys. Soc. Jpn.* **1958**, *13*, 880.
- (2) Sugano, S. *Suppl. Prog. Theor. Phys.* **1960**, *No. 14*, 66.
- (3) Sugano, S.; Peter, M. *Phys. Rev.* **1961**, *122*, 381.
- (4) Deutschbein, O. *Ann. Phys.* **1932**, *14*, 712.
- (5) Deutschbein, O. *Ann. Phys.* **1932**, *14*, 729.
- (6) Deutschbein, O. *Ann. Phys.* **1932**, *20*, 828.
- (7) Sugano, S.; Tsujikawa, I. *J. Phys. Soc. Jpn.* **1958**, *13*, 899.
- (8) Low, W. J. *Chem. Phys.* **1960**, *33*, 1162.
- (9) McClure, D. S. *J. Chem. Phys.* **1962**, *36*, 2757.
- (10) Margerie, J. C. R. *Hebd. Seances Acad. Sci.* **1962**, *255*, 1598.
- (11) Nelson, D. F.; Sturge, M. D. *Phys. Rev.* **1965**, *137*, A1117.
- (12) Powell, R. C.; DiBartolo, B.; Birang, B.; Naiman, C. S. *Phys. Rev.* **1967**, *155*, 296.
- (13) Fairbank, W. M., Jr.; Klauminzer, G. K.; Schawlow, A. L. *Phys. Rev. B* **1975**, *11*, 60.
- (14) Ballhausen, C. J. *Introduction to Ligand Field Theory*; McGraw-Hill: New York, 1962; p 103.
- (15) Pryce, M. H. L.; Runciman, W. A. *Discuss. Faraday Soc.* **1958**, *26*, 34.

- (16) Stevens, K. W. H. *Proc. R. Soc. London* **1954**, *A219*, 542.
- (17) Macfarlane, R. M. *J. Chem. Phys.* **1963**, *39*, 3118.

Table I. Calculated and Observed Transition Energies for $\text{Cr}^{3+}:\text{Al}_2\text{O}_3$ (cm^{-1})

excited state	obsvd ^a	Sugano ^b	Macfarlane ^c	Veremeichik ^d	this work ^e
ZFS	0.38 ^f	0.06	0.31 ^g		0.38
2E_g	14 418	13 550	14 054	14 352	14 415
	14 447	13 576	14 077		14 437
a ${}^2T_{1g}$	14 957	14 219	14 611	15 012	15 006
	15 168	14 340	14 807	15 112	15 070
	15 190	14 358	14 817		15 109
${}^4T_{2g}$	18 000 σ		17 924	17 877	18 007
			17 936		18 019
			17 966		18 247
			17 985		18 302
	18 400 π		18 411	18 311	18 339
			18 415		18 375
a ${}^2T_{2g}$	20 993	21 643	21 590	21 062	21 072
	21 068	21 749	21 614		21 109
	21 357	22 055	21 887	21 393	21 473
a ${}^4T_{1g}$	24 300 σ		24 431	24 238	24 520
			24 436		24 529
			24 438		24 548
			24 442		24 556
	25 100 π		25 587	25 261	24 668
			25 590		24 670
${}^2A_{1g}$	29 425			30 299	30 231
b ${}^2T_{2g}$	32 500 π			32 482	32 614
					32 679
				32 900	32 687
c ${}^2T_{1g}$	32 550 σ			32 756	33 062
				33 036	33 104
					33 119
b ${}^2T_{1g}$	36 700 π			37 392	37 561
	37 100 σ			37 865	37 688
					37 717
b ${}^4T_{1g}$	39 000 σ		39 326	39 031	38 239
			39 330		38 268
			39 381		39 248
			39 391		39 288
	39 000 π		39 413	39 189	39 317
			39 426		39 342
c ${}^2T_{2g}$	41 100 σ			41 426	41 593
					41 664
	41 100 π			41 899	41 717
2A_2	41 894			43 393	43 453

^a Reference 13. ^b Reference 3. ^c Reference 17. ^d Reference 20. ^e $\Delta_O = 23\,189 \pm 25$, $e_{\text{PO}} = 853 \pm 23$ ($e_{\text{PO}} = 8867$), $e_{\text{Al}} = -9275 \pm 18$, $B = 696 \pm 1$, $C = 2817 \pm 2$, $\alpha_T = 127 \pm 1$, $\zeta = 226 \pm 1$ (all in cm^{-1}). ^f Reference 11. ^g Macfarlane, R. M. *Phys. Rev. B* **1970**, *1*, 989.

Fairbank et al.¹³ attempted to improve Macfarlane's calculations by including a Trees correction, which takes the form $\alpha_T L(L+1)$ in the weak field basis set,¹⁸ in the Hamiltonian, a procedure that has also been found to be necessary in treating the free ion spectrum.¹⁹ This improved the overall fitting of the term energies; however, Fairbank did not include spin-orbit coupling in the Hamiltonian and therefore was unable to calculate the zero-field splitting or energies of all components of the sharp ${}^4A_{2g} \rightarrow \{{}^2E_g, {}^2T_{1g}, {}^2T_{2g}\}$ transitions. Apparently an optimization procedure was used to find a global minimum, although the procedure was not mentioned.

In 1986 Veremeichik²⁰ sought to improve Fairbank's calculations by including another correction term in the Hamiltonian of the form βQ ,²¹ where Q is the position operator. The Trees correction simulates configuration interaction of d^n with even configurations, while βQ simulates interactions with odd configurations. The calculations were performed in C_3 rather than C_{3v} symmetry as a mathematical artifice to partially express the effects of the Q operator. Again, however, spin-orbit coupling was neglected. An optimization procedure due to Polak and Skokov²²

was used to find the global minimum in a least-squares error function. The results from this seven-parameter model are shown in Table I.

The sharp-line splittings within the 2E_g , ${}^2T_{1g}$, and ${}^2T_{2g}$ states, which can only be modeled when spin-orbit coupling is part of the framework, can be sensitive indicators of the geometry of the metal ion environment.²³ These splittings are also known more accurately than the remainder of the spectroscopic data for ruby, except for the zero-field splitting. An appropriate model for the ruby system should therefore include spin-orbit coupling, and as Sugano and Macfarlane argued,^{3,17} the sharp-line splittings should be accorded considerable weight in the evaluation of geometry-related parameters, such as the trigonal field parameters.

The role of the trigonal field parameters is also worthy of reexamination. There is no doubt that they provide a particularly efficient means to express the overall ligand field potential with the minimum number of parameters. The problem lies in their lack of explicit chemical significance, the consequent impossibility of defining meaningful bounds for the parameter values, and the related lack of a direct relationship between the magnitudes of particular trigonal distortions and the trigonal field parameters. Elongation or compression along the C_3 axis or rotational displacement of the coordination triangles above and below the metal ion can lead to substantial changes in the trigonal field parameters that cannot be readily predicted, although Schoenen and Schmidtke have explored the empirical relationship at length.²⁴

In this paper we therefore make use of the angular overlap model (AOM) formalism, the parameters of which are geometry-independent.²⁵ In this treatment the ligand field potential is accumulated additively from perturbations by as many atoms as one may wish to include. Geometric factors for each atom appear in the ligand potential and can be evaluated explicitly when the geometry is known. In principle, the number of parameters necessary to describe the ligand field is considerably larger than the minimum. In ruby the chromium ion d orbitals are perturbed by oxide ions and aluminum ions at various distances. The adjustable parameters would include the AOM parameters e_σ and e_π for both O^{2-} and Al^{3+} and at least one parameter for each ion to account for the variation in the AOM parameters with distance. After subtraction of one parameter to be arbitrarily fixed (because only energy differences are measured), this leaves a minimum of five parameters and an effective redundancy. The five parameters in this model cannot, however, be set into analytical correspondence with the three trigonal field parameters. Furthermore, rather strict bounds can be set for all the parameters in the present model, so that the actual degree of mathematical redundancy is slight. As will be seen, the parameter set can be fortuitously reduced in the case of ruby, so that even this degree of redundancy is reduced or eliminated.

The application of the AOM has in the past been restricted to molecular complexes (or first coordination spheres), no doubt largely because of the difficulties in effectively parametrizing perturbing ions over a range of distances. There is therefore little upon which to base expectations for the values of the AOM parameters for O^{2-} and Al^{3+} . One goal of this work was to evaluate the effectiveness of an AOM approach to the development of the ligand field. A second was to assess the usefulness of the chemical information implicit in the values of the resulting AOM parameters.

Theory and Calculations

Geometry of the Chromium Site. The aluminum site in corundum (space group $R\bar{3}c$) has C_3 symmetry. The Al^{3+} ions lie closer to one triangle of oxide ions than the other, and the two triangles are twisted slightly away from the antiprismatic orientation, though still centered, of course, on the symmetry axis.²⁶ Chromium substitutes isomorphously

(18) Trees, R. E. *Phys. Rev.* **1951**, *83*, 756.

(19) Noorman, P. E.; Schrijver, J. *Physica* **1967**, *36*, 547.

(20) Veremeichik, T. F.; Grechushnikov, B. N.; Kalinkina, I. N. *Zh. Prikl. Spektrosk. (Engl. Transl.)* **1986**, *44*, 620.

(21) Rajnak, K.; Wybourne, B. G. *Phys. Rev.* **1963**, *132*, 280.

(22) Polak, B. G.; Skokov, V. A. *Standard Programs for Minimization of a Many-Variable Function*; Mosk. Gos. University: Moscow, 1967 (in Russian).

(23) Hoggard, P. E. *Coord. Chem. Rev.* **1986**, *70*, 85.

(24) Schoenen, N.; Schmidtke, H.-H. *Mol. Phys.* **1986**, *57*, 983.

(25) Schäffer, C. E. *Struct. Bonding* **1968**, *5*, 68.

(26) Moss, S. C.; Newnham, R. E. *Z. Kristallogr.* **1964**, *120*, 359.

Table II. Cartesian Coordinates for the 6 Oxide and 14 Aluminum Ions Closest to Chromium in Ruby (in Å)^a

	x	y	z	dist to Cr
O ²⁻ ^b	1.651	-0.111	0.708	1.800
	-0.922	-1.374	0.708	1.800
	-0.729	1.485	0.708	1.800
	0.729	1.263	-1.458	2.062
	0.729	-1.263	-1.458	2.062
	-1.459	0.000	-1.458	2.062
Al ³⁺ ^c	-1.828	-1.829	-1.829	2.783
	1.923	1.922	1.922	3.714
	-1.701	-1.701	1.665	2.817
	1.666	-1.701	-1.701	2.817
	-1.701	1.665	-1.701	2.817
	1.793	1.794	-1.572	3.154
	1.793	-1.572	1.794	3.154
	-1.573	1.794	1.794	3.154
	-0.170	-0.170	3.195	3.419
	3.196	-0.171	-0.171	3.419
	-0.170	3.195	-0.170	3.419
	-0.427	-0.427	-3.793	3.583
	-0.427	-3.793	-0.427	3.583
	-3.793	-0.427	-0.427	3.583

^a From crystal structure data of ref 27. ^b The z axis is the trigonal axis. ^c Origin is shifted by +0.385 Å along the z axis and coordinates are rotated to emphasize the near-cubic geometry of the first eight Al³⁺ values listed.

for aluminum in ruby, but the location of the Cr³⁺ ion is shifted by 0.13 Å along the C₃ axis toward the nearer oxide ion triangle.²⁷ The site symmetry is still C₃. The positions of the nearest six oxides are given in cartesian coordinates in Table II with the z direction chosen along the C₃ axis. Cartesian coordinates for the 14 nearest aluminum ions are also listed in Table II, but these have been rotated and shifted to emphasize their nearly cubic geometry.

Ligand Field Calculations. The methods for deriving the ligand field potential from a set of perturbing atoms in any geometry, and for determining the eigenvalues and eigenfunctions of a d³ ion in that field, have been described elsewhere.^{23,25} In substance, the metal ion d orbitals are rotated such that the d₂ orbital points directly at each perturbing atom in succession. That atom raises the energy of the (rotated) d₂ orbital by e_σ. If the π-interaction is cylindrically symmetrical, then the d_{xz} and d_{yz} orbitals are each raised in energy by e_π. If the π-interaction is restricted to a plane, as when originating from a single ligand p orbital, then the d orbital set is further rotated around the (new) z axis such that that interaction affects the d_{yz} orbital only. Finally, the d orbitals are rotated back to their original positions, spreading the interactions among all of them. The accumulation from all perturbing atoms results in the 5 × 5 ligand field potential matrix, ⟨d_i|V|d_j⟩.²³

To evaluate eigenvalues and eigenfunctions for a d³ ion, the full set of 120 single-term, strong field, antisymmetrized product wave functions was used as a basis. We have used the Hamiltonian function

$$\mathcal{H} = \sum_{i < j} \frac{e^2}{r_{ij}} + V_{LF} + \zeta \sum_i l_i s_i + \alpha_T \sum_i l_i^2 + 2\alpha_T \sum_{i < j} l_i l_j \quad (1)$$

which includes, in addition to the ligand field potential V_{LF}, interelectronic repulsion, a Trees correction in the functional form of orbit-orbit repulsion (last two terms), and spin-orbit coupling. The evaluation of matrix elements over each of these terms has been discussed previously.²³

The adjustable parameters in this treatment are the Racah parameters B and C, representing interelectronic repulsion, the Trees correction parameter α_T, the spin-orbit coupling parameter ζ, and a number of ligand field parameters, which must allow values of the AOM parameters e_σ and e_π to be assigned to each perturbing ion.

Unlike the case for a molecular metal complex, there is no fundamental distinction in an ionic lattice such as corundum between the atoms in the nearest coordination sphere (which might normally be called ligands) and those of the same type but further away. There is also no particular distance from the metal ion that could be said to logically define a sphere containing the most important perturbing ions. Besides the perturbations from oxide ions, the aluminum ions must also be considered. The nearest Al³⁺ ion lies 2.78 Å from Cr³⁺, much closer than the usual counterion distances in molecular complexes. The magnitude of the interaction of the Al³⁺ ions with the Cr³⁺ d orbitals is unknown

in terms of the AOM destabilization parameters, although the much smaller effects of K⁺ ions at larger distances have been examined.²⁸

Although in principle the field from a point charge can be put into equivalence with a combination of σ- and π-interactions,²⁹ we have assumed, as was done previously,²⁸ that the orbital structure of the Al³⁺ ion (4p higher in energy than 4s) makes the π-interaction negligible at all distances. Thus e_{πAl} was set equal to zero, which also performs the arbitrary fixing of orbital energies discussed above. Because of the complex and nonlinear relationship between the ligand field parameter set described here and the minimum set above, the arbitrary fixing is not actually required. The e_{πAl} parameter can be refined. However, when this was done, it always converged toward zero, which lends support to the assumption that the π-interaction is unimportant. The σ-interaction of Al³⁺ was represented by the parameter e_{σAl}. It is difficult to put a priori bounds on the value of e_{σAl} (vide infra), but it must be negative; i.e., the interaction with Al³⁺ lowers the energy of the Cr³⁺ d electrons.

The oxide ion interaction was represented by the AOM parameters e_{σO} and e_{πO}. The π-interaction was considered to be isotropic, although the oxide ion coordination sphere will in some sense lower the cylindrical symmetry of the Cr³⁺-O²⁻ interaction. Oxide was expected to be a strong σ-donor ion, for which e_σ could be expected to be in the 8000–11 000 cm⁻¹ range. We also expected that oxide would be a strong π-donor ion, stronger than OH⁻, for which e_π is about 2000 cm⁻¹.³⁰

The main problem in bringing the AOM treatment into play lies with the variation in the values of the AOM parameters with the distance from the Cr³⁺ ion. It is impractical to set separate, independent values for ions at different distances. In the past we have modeled the distance dependence of the AOM parameters on that for the classical field from a single point charge, which yields only R⁻³ and R⁻⁵ terms.^{28,29,31} Thus

$$e_{\lambda Z} = aR^{-3} + bR^{-5} \quad (\lambda = \sigma, \pi; Z = \text{Al, O}) \quad (2)$$

When e_{λZ} at the nearest ligand position, R_{0Z}, is used as a reference value, e_{λZ}⁰, the expression for e_{λZ} at distance R_Z, becomes

$$e_{\lambda Z} = e_{\lambda Z}^0 \left\{ \frac{R_{0Z}^{-3} + \frac{b}{a} R_{0Z}^{-5}}{R_Z^{-3} + \frac{b}{a} R_Z^{-5}} \right\} \quad (\lambda = \sigma, \pi; Z = \text{Al, O}) \quad (3)$$

The ratio (b/a) was assumed to be the same for e_{σO} and e_{πO}. This left two adjustable parameters to represent the dependence on distance, (b/a)_{Al} and (b/a)_O. The assumption that the R⁻³ and R⁻⁵ dependences expected for point charges apply to the perturbing ions in ruby neglects electron cloud (Born) repulsion, which could introduce one or more additional R⁻ⁿ (n = 6–12) dependences for the nearest ions. There may be good cause to doubt the validity of the radial dependence implied by crystal field theory;³² however, the guiding principle for the present calculations was simplicity. The radial dependence was to be expressed with as little additional parametrization as possible, even at the expense of a better fit to experiment. Crystal field theory is a reasonable starting point, although a more accurate radial dependence may ultimately be found.

Thus, the initial parameter set consisted of five parameters to model the ligand field (e_{σAl}, e_{σO}, e_{πO}, (b/a)_{Al}, and (b/a)_O) plus the parameters taken from the treatment of the free ion (B, C, α_T, and ζ). A total of 813 O²⁻ and 542 Al³⁺ ions were included in the ligand field. The e_σ values of the most distant ions in this set were below 20 cm⁻¹. This set included all oxide and aluminum ions within approximately 15 Å of the chromium center. Eigenvalues were determined by diagonalization of the full 120 × 120 Hamiltonian matrix. The best fit to the experimental energies was found by means of the Powell parallel subspace optimization procedure.^{33,34} The function minimized was

$$f = \sum Q^2 + 10^2 \sum D^2 + 10^3 \sum S_T^2 + 4 \times 10^3 \sum S_E^2 + 10^5 \sum Z^2 \quad (4)$$

where Q, D, S_T, S_E, and Z represent the differences between the experimental and calculated quartet energies (⁴T_{2g} and the first ⁴T_{1g}), doublet energies, the overall ²T_{1g} and ²T_{2g} splittings, the ²E_g splitting, and the ground-state zero field splitting, respectively. The weighting factors in this function are in approximate proportion to the inverse squares of the

(28) Hoggard, P. E.; Lee, K.-W. *Inorg. Chem.* **1988**, *27*, 2335.

(29) Schäffer, C. E. *Struct. Bonding* **1973**, *14*, 69.

(30) Schläfer, H.-L.; Martin, M.; Schmidtke, H.-H. *Ber. Bunsen-Ges. Phys. Chem.* **1971**, *75*, 787.

(31) Smith, D. W. *J. Chem. Soc. A* **1969**, 1708.

(32) Powell, M. J. D. *Comput. J.* **1964**, *7*, 155.

(33) Kuester, J. L.; Mize, J. H. *Optimization Techniques with FORTRAN*; McGraw-Hill: New York, 1973.

(34) Clifford, A. A. *Multivariate Error Analysis*; Wiley-Halstad: New York, 1973.

(27) Tselison, V. G.; Antipin, M. Y.; Gerr, R. G.; Ozerov, R. P.; Struchkov, Y. T. *Phys. Status Solidi A* **1985**, *87*, 425.

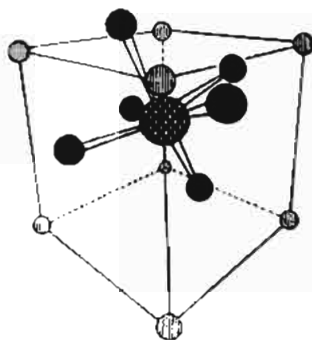


Figure 1. Representation of a Cr^{3+} ion in ruby surrounded by six oxide ions (in dark shading) and a distorted cube of eight aluminum ions (shown in outline). Six more Al^{3+} ions are located approximately at the centers of the cube faces.

corresponding experimental uncertainties.

In the course of initial optimizations, the value of $(b/a)_O$ tended toward zero, while $(b/a)_{Al}$ optimized at about 75 \AA^2 . In approximate terms this means that the oxide ion AOM parameters exhibit only an R^{-3} dependence. The factor of 75 for the aluminum ions does not imply a strict R^{-5} dependence, however. The values of (b/a) in eqs 2 and 3 represent the ratio of the R^{-3} contribution to the R^{-5} contribution only when R^{-3} is numerically equal to R^{-5} , i.e., at $R = 1 \text{ \AA}$. At larger distances the R^{-3} term eventually gains dominance, unless (b/a) is quite large. The factor of 75 for Al^{3+} means that the R^{-5} term is larger for the nearest aluminum ions, but the R^{-3} term would be larger beyond $R = 8.7 \text{ \AA}$. There is some sense to this, in that the nearest 14 aluminum ions form a more symmetric environment around the chromium center than do the nearest six oxide ions. The near- Al^{3+} environment can be represented as a distorted cube, with eight ions at the corners (see Table II) and six on the faces. This is shown graphically in Figure 1. In cubic symmetry a strict R^{-5} dependence would apply in crystal field theory. The near- O^{2-} environment is much further from the octahedral symmetry that would be required to eliminate the R^{-3} dependence.

It is still not clear why the R^{-3} dependence should in effect vanish entirely for the O^{2-} ions. An R^{-3} dependence alone has been found to model effectively the field from counterions in a low-symmetry arrangement,²³ but the nearest O^{2-} ions are much closer to the metal ion in the case of ruby, and the discrepancy between the distances to the two triangles in the nearest set of oxides is the leading factor in reproducing the experimental sharp-line splittings, so any R^{-3} dependence within that range of distances would still be important even when the whole 813 atom set is considered.

In any case the limiting, or near-limiting, values for (b/a) made it possible to assume a straight R^{-3} dependence for e_{eO} and e_{eAl} , dropping the $(b/a)_O$ term as a parameter. We also chose to ignore the R^{-3} dependence for Al^{3+} rather than refine $(b/a)_{Al}$. This is more of an approximation for Al^{3+} than that made for the O^{2-} ions but is less significant than other approximations, such as the isotropic treatment of the oxide ion interaction. This reduced the number of adjustable ligand field parameters to three and the total number of parameters varied during optimization to seven.

Once again, the distance parameters were eliminated solely for simplification, intentionally sacrificing a mathematically better fit. In fact, the distance dependence could well be still more complicated than we have outlined, both on theoretical grounds³⁵ and from the practical consideration that the inner and more distant coordination spheres may follow completely different distance dependences. That a simplification to a single nonparametric distance dependence for each of the two ion types was practical should not be taken to mean that the functional form of eq 2 is correct. Other functional forms, such as a $\exp(-bR/R_0)$, yielded fits that were as good or better but at the cost of additional adjustable parameters.

Results and Discussion

The results of this optimization are presented in the last column of Table I. Although only the ${}^4A_{2g} \rightarrow {}^2E_g, {}^2T_{1g}, {}^2T_{2g}, {}^4T_{2g}, {}^4T_{1g}$ transition energies were used in the optimization, the higher excited states, as assigned by Fairbank et al.,¹³ were also fit reasonably well by the same parameter set. One should bear in mind, however, that Fairbank's assignments from excited-state absorption spectra were not based on direct experimental evidence but were

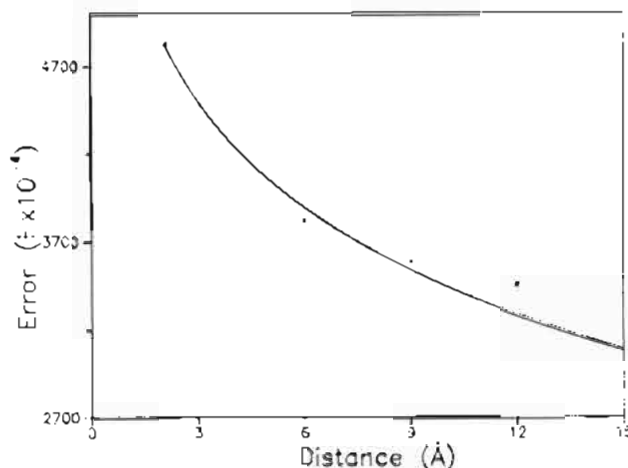


Figure 2. Variation of least-squares error (eq 4) with distance from Cr^{3+} of ions included in the ligand field potential. An optimization was performed at each point.

matched to calculated transition energies.

The calculated transition energies fit the experimental values much better than do Macfarlane's due to two factors: our use of a Trees correction, which has the effect of allowing the average term energies to be better fit, and our use of a reliable optimization procedure to find the global minimum in the error function of eq 3. The development of the ligand field in terms of distance-dependent AOM parameters yields chemically more meaningful information but cannot increase the range of possibilities over Macfarlane's symmetry-adapted procedure and in fact decreases the range. By transformation of the basis set for the ligand field potential matrix to the complex trigonal basis used by Tanabe and Sugano and by Pryce and Runciman,³⁶ the equivalent values of the trigonal field parameters v and v' were found to be -799 and $+76 \text{ cm}^{-1}$.

Veremeichik's calculated transition energies are not directly comparable, since spin-orbit coupling was not included in those calculations, and so not all of the sharp-line splittings could be calculated. With respect to average term energies, our results appear to be no worse than Veremeichik's. The main difference would appear to lie in the error functions used for optimization. Equation 4 weights the sharp-line transitions (to the ${}^3E_g, a {}^2T_{1g}$, and $a {}^2T_{2g}$ states) heavily, and these are correspondingly better fit by our procedure. We did not use the correction term βQ in the Hamiltonian, as Veremeichik did, but it does not seem to have affected the closeness of the fit.

The least-squares error f (eq 4) represented by the calculated energies in Table I was 2.9×10^7 . When fewer ions were included, the fitting error was larger. This is illustrated in Figure 2, which shows a plot of the least-squares error, optimized separately for each point, as a function of the distance from the chromium ion of the outermost ions included in the ligand field potential. The first point in Figure 2 included the nearest six oxide and eight aluminum ions. An alternative calculation was tried in which only the six nearest oxygens were used to develop the ligand field potential, while the π -interaction was allowed to be anisotropic ($e_{\pi x} \neq e_{\pi y}$), in an attempt to use this device to account for the remainder of the crystal field. The least squares error was much higher, 1.6×10^8 . It is possible that separate AOM parameters for the two sets of equivalent oxygens would more successfully model the entire field, but we feel that this introduces too many adjustable parameters into the calculation.

The optimized parameter set is also shown in Table I. The error limits given are those resulting from the error propagated by average experimental uncertainties of 30 cm^{-1} for the quartets, 3 cm^{-1} for the doublets, 1 cm^{-1} for the 2T term splittings, 0.5 cm^{-1} for the 2E_g splitting, and 0.01 cm^{-1} for the zero-field splitting. The

(35) Pueyo, L.; Bermejo, M.; Gomez-Beltran, F. *Anal. Quim.* 1980, 76, 180.

(36) Pryce, M. H. L.; Runciman, W. A. *Discuss. Faraday Soc.* 1958, 26, 34.
(37) Lee, K.-W.; Hoggard, P. E. *Inorg. Chem.* 1988, 27, 907.

Table III. Correlation Coefficients Derived from the Optimization of Table I

$e_{\sigma O}$	$e_{\pi O}$	$e_{\sigma Al}$	B	C	ζ	α_T
1.000	0.972	0.863	-0.303	-0.046	-0.904	0.423
	1.000	0.803	-0.307	0.075	-0.929	0.315
		1.000	-0.234	-0.249	-0.588	0.564
			1.000	-0.674	0.318	-0.366
				1.000	-0.157	-0.386
					1.000	-0.230
						1.000

value of $e_{\sigma O}$ (8867 cm^{-1}) is within the range of expectation. Values of 8300–8600 cm^{-1} have been assigned to $e_{\sigma O}$ for some hydroxo complexes of Cr(III).³⁰ However, $e_{\pi O}$ (853 cm^{-1}) turned out to be smaller than expected. Hydroxide has been assigned values of $e_{\pi O}$ between 1700 and 2900 cm^{-1} ,³⁰ and oxygen ligands in general, particularly when they possess a negative charge, are generally considered to be strong π -donors.

The reason for this discrepancy lies in the nature of the oxide ligand in an ionic crystalline lattice, in which it effectively shares its donor characteristics with its entire coordination sphere. The values for the hydroxo ligand mentioned above refer to molecular complexes, in which each ligand affects primarily one metal ion. In corundum each O^{2-} has four Al^{3+} nearest neighbors, two 1.86-Å and two 1.97-Å distant. The Al–O–Al angles are 85, 94, 120, and 132°. These angles are slightly altered when one ion in the coordination sphere is a Cr^{3+} . If the four Al^{3+} ions formed a perfect tetrahedron, the O^{2-} ion could be considered to interact with σ -symmetry with each Al^{3+} (or Cr^{3+}) through a lone pair, leaving no π -interaction. In the actual distorted tetrahedron most of the O^{2-} electron density is apparently still used for direct σ -interaction, and the residual π -interaction felt by the Cr^{3+} ion can be attributed to the slight overlap of a misdirected set of tetrahedrally oriented oxide lone pairs with the Cr^{3+} d_{xz} and d_{yz} orbitals (after rotation to point the d_{z^2} orbital at the oxide). Note also that the value of $\Delta_O = 3e_{\sigma O} - 4e_{\pi O}$ that would be derived from Table I for the oxide ion (23 189 cm^{-1}) cannot be equated directly with any particular spectral feature, since the oxides are shared, and the manner of their sharing affects the distribution of the electron donor characteristics of oxide between e_{σ} and e_{π} . The quartet transition energies, especially the ${}^4A_{2g} \rightarrow {}^4T_{2g}$ energy, depend directly on Δ in crystal field theory, but this latter Δ depends on the entire environment of the metal ion, including aluminum ions.

By any of several criteria the value of $e_{\sigma Al}$ (–9206 cm^{-1}) seems too large, though it at least has the correct sign for an interaction that stabilizes the Cr^{3+} d electrons. If the R^{-5} distance dependence is used to project this value to 1.800 Å, the distance of the closest oxide ions, an e_{σ} of –80 000 cm^{-1} is obtained. Alternatively, the oxide ligand field at 2.78 Å, the distance of the nearest aluminum ions, would be $e_{\sigma O} = 2400$ and $e_{\pi O} = 230$ cm^{-1} . The value of $e_{\sigma Al}$ is very large, even considering the higher charge on the aluminum ion. We would suggest that the crystal fields of Al^{3+} and O^{2-} cannot be evaluated equivalently, because the closer oxide ions interact with the metal ion both covalently and electrostatically, while the aluminum ions provide a more strictly electrostatic perturbation. The same sort of difference may exist between the nearest oxides and those further away, but we are unable to assess this because we did not model these groups separately.

Because the crystal field Δ depends on all three of the AOM parameters [$e_{\sigma O}$, $e_{\pi O}$, $e_{\sigma Al}$], and is more or less fixed by the position of the first spin-allowed band (${}^4A_{2g} \rightarrow {}^4T_{2g}$), there is a high degree of correlation among these three parameters, which is shown in Table III. Thus, if $e_{\sigma O}$, for example, were arbitrarily raised in

value, either $e_{\pi O}$ or $e_{\sigma Al}$ would have to rise as well in order for the ${}^4A_{2g} \rightarrow {}^4T_{2g}$ transition energy to stay approximately constant. If the site symmetry were octahedral, the correlation would be complete. A partial decoupling can be effected by using [Δ_O , $e_{\pi O}$, $e_{\sigma Al}$] as the parameter set, with Δ_O defined as above, but the optimization results are the same.

The other parameters fall well within their expected bounds. The parameters B , C , and ζ are all smaller than their free ion values, and α_T is larger, as it is in all cases where optimizations have been performed on a set of transition energies that included at least all the t_{2g}^3 components.^{20,23,28,36} The spin-orbit coupling parameter ζ in particular is much more precisely fixed than it typically has been in models of molecular complexes,^{23,28} in large part because of the inclusion of the zero-field splitting in the fitting process, and the value of 226 cm^{-1} may be suitable when ζ must be arbitrarily fixed.

Conclusion

An AOM parametrization has successfully represented the ligand field potential in an ionic crystal, which might be taken as the least likely venue for the angular overlap model, because of the potentially large number of parameters involved. The procedure we used makes no explicit use of symmetry, but does so implicitly by factoring in the exact geometry of each perturbing ion. Once the model was set up, the number of ions to be included in the ligand field potential was arbitrary, involving no new adjustable parameters. With a minimal environment of 6 O^{2-} ions and 14 Al^{3+} ions used in the beginning, the error was continuously reduced as shells of more distant ions were added and the optimization repeated. Presumably, the agreement with experiment would improve still further if more shells were included beyond the set of 813 O^{2-} and 542 Al^{3+} we have used for this paper, although that improvement should be small.

The AOM treatment of the ligand field potential in an ionic crystal also provides a window to the important question of the dependence of the AOM parameters on the distance from the metal ion. Except for the special case of the cubic symmetry groups, for which the distance dependence is straightforwardly predicted by crystal field theory to be R^{-5} ,³⁸ little is known and little can be predicted. Hecht has calculated and compared relative values for a and b of eq 2 in different angular geometries,³⁹ but the coefficients are arbitrary as far as the metal–ligand distance is concerned. We used Hecht's program to examine separately the coefficients from the angular geometry of the nearest 6 oxide ions and the nearest 14 aluminum ions. The Al^{3+} set yielded a strong dominance by the R^{-5} coefficient, while the R^{-5} coefficient was also larger than the R^{-3} coefficient for the O^{2-} set, though not by as much. Even though the magnitudes of these coefficients are without quantitative meaning, and only the closest ions were evaluated, it was still unexpected to find the R^{-5} dependence for O^{2-} nearly vanishing during the optimization procedure. The question of distance dependence is far from settled, but the methods outlined here provide an empirical means to assist in evaluating this in other systems.

Acknowledgment. This material is based upon work supported in part by the National Science Foundation under Grants RII8610675 and CHE8815829. We also thank the donors of the Petroleum Research Fund, administered by the American Chemical Society, for support of this work.

Registry No. Al_2O_3 , 1344-28-1; Cr, 16065-83-1; ruby, 12174-49-1.

(38) Schmidtke, H.-H. *Quantenchemie*; VCH Verlag: Weinheim, FRG, 1987; p 264.

(39) Hecht, H. G. *Comput. Chem.* **1985**, *9*, 295.